國立臺灣大學電機資訊學院資訊工程學系
碩士論文
Department of Computer Science and Information Engineering
College of Electrical Engineering and Computer Science
National Taiwan University
Master Thesis

藉由環繞於頭部周遭的慣性力式規律震動回饋增進虛擬實境動態體驗

DrivingVibe: Enhancing VR Motion Experience with Inertia-based Vibrotactile Feedback Patterns around the Head

林琮珉
Tsung-Min Lin

指導教授：陳彥仰博士
Advisor: Mike Y. Chen, Ph.D.

中華民國 111 年 9 月
September, 2022

doi:10.6342/NTU202203767

國立臺灣大學碩士學位論文
口試委員會審定書

藉由環繞於頭部周遭的慣性力式規律震動回饋增進虛擬實境動態體驗

DrivingVibe: Enhancing VR Motion Experience with Inertia-based Vibrotactile Feedback Patterns around the Head

本論文係林琮珉君（學號 R09922167）在國立臺灣大學資訊工程學系完成之碩士學位論文，於民國 111 年 9 月 20 日承下列考試委員審查通過及口試及格，特此證明

口試委員：

陳彥仰 (Sep 20, 2022 15:45 GMT+8)

（指導教授）

鄭龍磻 (Sep 20, 2022 15:45 GMT+8)

蔡欣叡 (Sep 20, 2022 20:57 GMT+8)

系 主 任

誌謝

首先，感謝陳彥仰教授願意接受一個沒有相關背景的備取生進入實驗室，在這兩年期間提供非常多的指導與研究上的建議，也打造出很友善且輕鬆的實驗室環境，讓學生能在最佳的狀態下做研究。

也感謝余能豪教授，老師在此研究上給出了非常多的導引，更大方的提供貴實驗室的資源幫忙，沒有您也不會有這篇研究的存在。

感謝口試委員鄭龍磻教授、陳炳宇教授、和蔡欣叡教授，委員們專程撥冗出席我們的學位考試，也在當下針對我們的論文與研究提出許多見解與可能的發展，這些都是非常寶貴的意見。

感謝所有參與過這個研究的成員，謝謝世宇這兩年來的協助，硬體設計、照片與影片的拍攝剪輯這些我不拿手的部分，你都幫了非常大的忙；謝謝佳霖、中瑋、紹瑜早期對於研究建立的貢獻；謝謝嘉安、采媛、Luca、雅淇、姿穎在研究上的幫助，有你們的人力才能順利完成。

感謝筠庭在投稿時的協助，論文中的數據圖表能這麼精美是你的功勞；也一併感謝詩芩、青邑、柏佑在這兩年學涯上的陪伴，跟你們一起當實驗室同伴是很快樂的事；感謝羿宣、雨新、雋淼學長姐在進入實驗室時給予諸多的帶領，更謝謝佑威學長在硬體設計上的啟發與幫忙，你是我們的光芒。

最後，感謝我的父母、兩位哥哥、還有朋友們在生活各方面的支持與鼓勵，讓我能夠有動力在這條路上向前不懈，謝謝你們。

doi:10.6342/NTU202203767

摘要

我們提出 DrivingVibe，探索如何利用環繞於頭部周遭的震動回饋設計去增進虛擬實境中的行車動態體驗。在整個設計流程之中，我們完成了三個裝置設計的迭代並進行了一系列共招募 66 名受測者的形成性與總結性研究，最後發展出兩套使用了 360 度震動觸覺頭帶的回饋規律設計：鏡像與 3D 慣性力式規律。鏡像設計延伸手持控制器的震動觸覺規律來均勻的驅動頭帶。3D 慣性力式設計則提供對應慣性力的方向性震動規律，包括：離心力、水平方向的加速度與減速度、以及粗糙地形導致的垂直移動。我們進行了一個 24 名受測者的使用者體驗評量研究，體驗內容包含被動的乘客模式與使用帶有震動回饋的手持控制器操作的主動駕駛模式。研究結果顯示兩套 DrivingVibe 的設計皆能顯著且效應大地增進體驗的真實感、沉浸感、與樂趣 (p 值 <.01)，在整體偏好的方面，88% 的使用者偏好 DrivingVibe，並且在這些人之中有 67% 的人偏好 3D 慣性力式設計。

關鍵字：遊戲/遊玩；觸覺；虛擬實境；感覺運動耦合；動態模擬器；頭部震動

doi:10.6342/NTU202203767

Abstract

We present DrivingVibe, which explores vibrotactile feedback designs around the head to enhance VR driving motion experiences. Throughout our design process, we completed three device design iterations and conducted a series of formative and summative user studies with a combined total of 66 participants. We arrived at two feedback pattern designs that use a 360°vibrotactile headband: 1) *mirroring* and 2) *3D inertia-based* patterns. The mirroring design extends the vibrotactile patterns of the handheld controllers to actuate the headband uniformly. The *3D inertia-based* design provides directional vibration patterns corresponding to inertial forces, including: i) centrifugal forces, ii) horizontal acceleration/deceleration, and iii) vertical motion due to rough terrain. We conducted a 24-person user experience evaluation in both passive passenger mode and active driving mode, with the active mode using handheld controllers with vibrotactile feedback. Study results showed that both DrivingVibe feedback designs significantly improved realism, immersion, and enjoyment ($p<.01$) with large effect sizes. In terms of overall preference, 88% of users preferred DrivingVibe, and among these users, 67% preferred the *3D inertia-based* design.

Keywords: Games/Play ; Haptic ; Virtual Reality ; Sensorimotor Contingency ; Motion simulators ; Head Vibrations

doi:10.6342/NTU202203767

Contents

doi:10.6342/NTU202203767

doi:10.6342/NTU202203767

List of Figures

doi:10.6342/NTU202203767

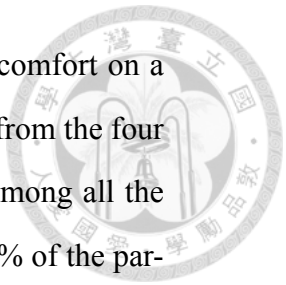

doi:10.6342/NTU202203767

List of Tables

doi:10.6342/NTU202203767

Chapter 1

Introduction

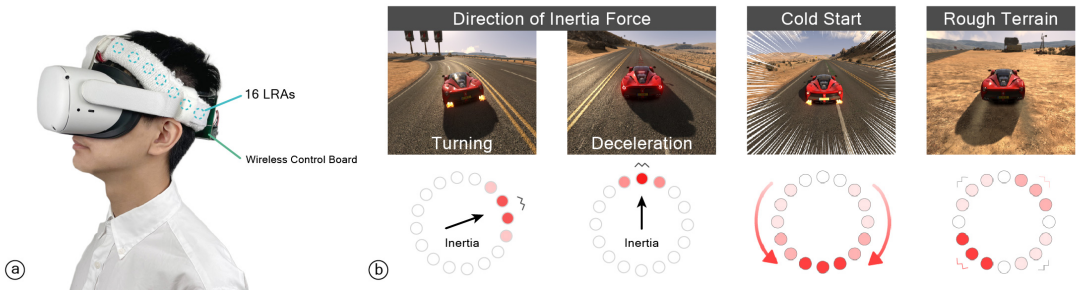

Figure 1.1: (a) The system of DrivingVibe can be integrated easily with VR headset and produces (b) inertia-based feedback patterns corresponding to the motion events, including *turning*, *deceleration*, *cold start*, and *rough terrain shaking*.

Haptic feedback enhances the realism, immersion, and enjoyment of virtual experiences. To enhance motion experiences, such as driving and flying, traditional motion platforms mechanically tilt and move the entire person, which requires large machinery. Even with the significant space and cost requirements, interest in consumer motion platforms has been growing rapidly along with VR headsets, particularly for driving and flight simulation.

To address the limitations of motion platforms, researchers have explored more compact designs and also wearable approaches to motion simulation. HapSeat [7] used three 3-DOF motorized actuators attached to seats to independently move users' heads and hands instead of the entire body. HeadBlaster [31] introduced the first wearable motion simulator by using air propulsion jets integrated into VR headsets but requires external air

doi:10.6342/NTU202203767

compressors. Odin's Helmet [18] used head-mounted propellers instead of air jets, but it is heavy and generates unsafe noise that exceeds 100dB. While these approaches eliminate the need for extensive mechanical platforms, they still impose significant usability, space, and cost barriers to consumer adoption.

Vibrotactile actuators, particularly Linear Resonant Actuators (LRAs), have been embedded in VR controllers and smartphones to provide haptic feedback. They are compact and lightweight and are starting to be integrated into VR headsets, such as the PlayStation VR2 (expected 2023). Researchers have also explored using head-mounted vibrotactile actuators with static and apparent tactile motion patterns to provide cues for navigation guidance [23] and to simulate teleportation in VR [5].

We present DrivingVibe, which explores vibrotactile feedback designs around the head to enhance VR driving experiences. Throughout our design process, we completed three device design iterations, and we conducted a series of two formative studies and a summative user study with a combined total of 66 participants (excluding pilot studies). We arrived at two feedback pattern designs using 360°vibrotactile headbands: 1) *mirroring* and 2) *3D inertia-based* designs. The *mirroring* design extends the vibrotactile patterns of the handheld controllers to actuate the headband uniformly. The *3D inertia-based* design provides directional vibration patterns corresponding to the direction of inertial forces in the X, Y, and Z axes.

Using a headband with 16 Linear Resonant Actuators (LRAs), we designed feedback patterns for the following four types of motion events: 1) turning, 2) acceleration/deceleration, 3) cold start and 4) vertical motion due to rough terrain. These types of motion events were selected as they were the most noticeable sensory events in driving experiences. Based on sensorimotor contingencies [9], which refers to the matching of particular patterns from multisensory information to actions, we designed the *3D inertia-based* feedback for each motion event using the following two types of vibrotactile patterns: 1) *directional cues* using a subset of LRAs, and 2) *motion cues* using apparent tactile motion [5], as shown in Figure 1.1. While DrivingVibe does not physically tilt users' heads to simulate inertia forces, prior studies have shown that applying vibrations

doi:10.6342/NTU202203767

to the head can stimulate the vestibular system [38, 58].

We conducted a 24-person user experience evaluation in both passive passenger mode and the active driving mode, with the active mode using handheld controllers with vibrotactile feedback. Study results showed that both DrivingVibe designs significantly improved realism, immersion, and enjoyment ($p<.01$) with large effect sizes. Also, participants rated DrivingVibe to be more comfortable, though the improvement was not statistically significant ($p>.05$). Regarding overall preference, 88% of users preferred DrivingVibe, and among these users, 67% preferred the *3D inertia-based* design.

Furthermore, DrivingVibe is lightweight and compact, and the entire system can be integrated into VR headsets, making it practical and suitable for consumer adoption. We will open-source the entire software and hardware of DrivingVibe so that others can experience and build upon our progress. The rest of the paper first reviews related research on motion simulation and applying haptic feedback to the head. We then discuss the vibration pattern designs and implementation and present user experience evaluation and discussion.

doi:10.6342/NTU202203767

Chapter 2

Related Work

Our work is clearly inspired by the rich body of prior work on motion simulation and head-based haptic feedback.

2.1 Motion Simulation Techniques

Historically, motion platforms were originally invented at the beginning of the 1900s for training pilots. Over time the actuation methods evolved from manual [17], to wind-based [43], to linear actuators [50], and their number of supported degrees of freedom (DoF) increased from 3-DoF (pitch, roll, and yaw) [1] to 6-DoF (rotational: pitch, roll, and yaw, translational: surge, heave, and sway) [50]. While motion platforms continue to be indispensable for training [2, 11], they have also become popular for entertainment [45] and for personal VR experiences, particularly for driving and flight simulation.

To reduce the space and machinery required by large, mechanical motion platforms, seat-based approaches such as HapSeat [7] and vibrotactile actuators have been explored for motion [16, 46, 61, 6, 29] and terrain texture [30, 32] simulation.

Headset-based motion simulation using compressed air jets, such as HeadBlaster [31] and HeadWind [54] have been shown to increase realism and immersion of motion and teleportation in VR, respectively. These approaches, however, require a source of compressed air provided by air compressors or portable air tanks. Odin's Helmet [18] uses head-mounted propellers, which are heavy, and its noise level at >100dB may be unsafe.

doi:10.6342/NTU202203767

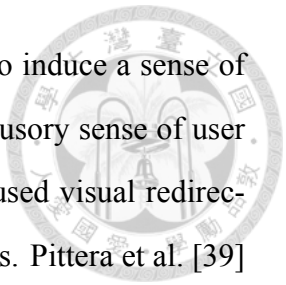

There have also been studies that aim to exploit illusory effects to induce a sense of motion. Väljamäe et al. [55] used auditory scene cues to create an illusory sense of user movement relative to the source of the sound, while VMotion [49] used visual redirection to maintain an illusion of unconstrained walking in limited spaces. Pittera et al. [39] explored if ultrasound haptics could induce an intermanual tactile illusion of movement.

This paper takes a different actuation approach to motion simulation by using vibrotactile actuators that can be easily integrated into consumer VR headsets to explore feedback designs that enhance motion experience. Despite vibrotactile actuators being limited in power and fidelity compared to larger, heavier, and nosier actuators that are effective but much less practical, we demonstrate that our approach and pattern designs can also significantly enhance the driving motion experience.

2.2 Haptic Feedback on the Human Head

Kabuto [53] and GyroVR [14] rendered impact and inertia through the use of head-worn flywheels and their gyroscopic effects. VaiR [42], AmbioTherm [40], ThermEarhook [36] and VWind [19] increased sense of presence and immersion using head-focused thermal and wind stimuli. Head-based force feedback [4], electrical-muscle-stimulation (EMS) [52, 51], lateral skin stretch [57]. Researchers have also explored feedback that focuses on the face, such as FaceHaptics [59], Virtual Whiskers [35], HeadWind [54], and Mouth Haptics [47]. While diverse in the types of haptic feedback these prior approaches can provide, they generally require significant hardware to be mounted on the headset and have not explored haptic designs for continuous motion simulation, such as driving.

Moreover, studies have shown that humans can recognize around-the-head spatial vibrotactile patterns with high accuracy [8, 24] and indicate that, depending on the vibrotactile localization, the funneling illusion may be perceivable in areas of the head [26]. ProximityHat [33], HapticHead [22, 23, 25], TactiHelm [56] and MotionRing [5] leverage these perceptual capabilities to deliver around-the-head directional cues for navigation in real world and virtual environments. While these approaches have explored vibrotactile and directional cues, they have not explored haptic designs for inertia forces nor continu-

doi:10.6342/NTU202203767

ous motion simulation.

Inspired by these prior work, this paper contributes a deep design exploration using practical, headset-integrated vibrotactile actuators to enhance motion experience, specifically driving.

doi:10.6342/NTU202203767

Chapter 3

Device Design and Implementation

We used an iterative design process for the device and for the vibrotactile pattern design. We developed three iterations of our device (V1-V3) and conducted two formative studies (n=24, 18) using V2 and V3 iterations of our devices. We improved the device and pattern design based on the feedback collected. We present our device design iteration in this section and vibrotactile feedback design iteration in the next section.

3.1 Device Design Iteration

We reviewed several types of vibrotactile actuators, including eccentric rotating mass (ERM), linear resonant actuator (LRA), Dielectric elastomers actuators (DEA), and piezo-electric actuators. ERM and LRA are the most commonly used actuators used in a gamepad and VR controllers and prior research headset devices [38, 5]; thus we selected them for availability, low noise, low cost, and ease of integration into VR headsets.

3.1.1 Device: V1 (4 x ERM)

As shown in Figure 3.1(a), our first prototype consists of 4 ERM motors (Parallax, 12mm coin type, 9000rpm) pressed into the sponge cushion of the Vive Pro HMD, controlled via an Arduino Nano board on the front of the HMD. It supports vibrotactile feedback in 8 directions by actuating one or two of the motors.

doi:10.6342/NTU202203767

3.1.2 Device: V2 (16 x LRA)

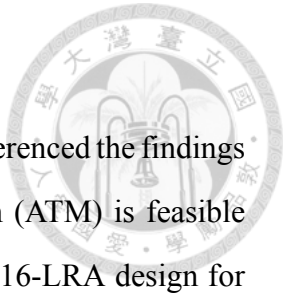

To increase the number of actuators for higher haptic resolution, we referenced the findings of MotionRing [5], which demonstrated that apparent tactile motion (ATM) is feasible on both 12-LRA and 16-LRA headband designs. We chose to use a 16-LRA design for higher haptic resolution, which has an angular spacing of $22.5°$. We initially used the same coin-type LRA as MotionRing but found that these LRAs often malfunctioned due to overheating in our more extended usage scenario. Therefore, we switched to the LRAs used by Nintendo Switch controllers (VL91022-170H, 22.6mm x-axis rect type), which can sustain the extended actuation that we needed, and also has the benefit of an 11x larger force magnitude of 2.3N (vs. 0.2N).

To make the LRAs easier to wear, we cut open an elastic sports headband and weaved 16 pockets inside the headband. Each actuator was then tucked into the pockets, such that the individual shape and location of actuators are not perceivable by users, while the vibrations are easily felt.

As shown in Figure 3.1(b), the 16 LRAs are controlled via 16 DRV2605L driver boards by a NodeMCU-32S on a perfboard, which was encased in an acrylic case and attached to the back of the VR headset. The LRA headband weighs 180g, while the board with the case weighs 262g and has a volume of $17 \times 9.5 \times 3.5\ cm^3$.

3.1.3 Device: V3 (Wireless)

Based on feedback from our formative studies, we made three key improvements to make it easier to wear and operate, as shown in Figure 3.1(c) and also Figure 1.1(a). First, we reduced the weight and volume of the control board by more than 80% to 45g and more than 70% to $10 \times 7.5 \times 2\ cm^3$, by custom designing a printed circuit board (PCB) to simplify the wiring. Second, we made the system wirelessly controlled via Wi-Fi, enabling full user mobility. Third, we improved the mounting of LRAs to the headband with double-sided tape, preventing unintended rotation during wearing and usage, which sometimes caused the LRA's actuating axis to deviate from being perpendicular to the surface of the head resulting in unpredictable intensity.

doi:10.6342/NTU202203767

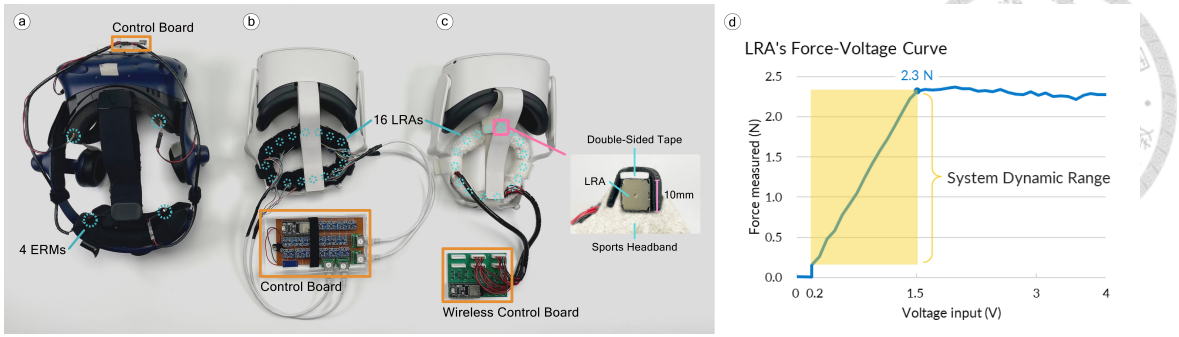

Figure 3.1: (a) V1 prototype (b) V2 prototype; (c) V3 device used in user experience evaluation; (d) Force output vs. input voltage for the LRA

3.2 LRA Amplitude and Response Time

We controlled the LRA voltage from 0-5V [48] and measured the force output using a IMADA ZTS-20N load cell, which can record data at 2000Hz at up to 20N and has a rated accuracy of 0.2% full scale (0.04N). As shown in Figure 3.1(d), the LRA generates force amplitude at 1.5N per volt input ($R^2 = 0.999$) from 0.2N up to 2.3N, which we use as the controllable dynamic range of the system.

The response time of the LRA to reach maximum amplitude is 10ms. The system updates the vibration state of the headband at a rate of 25Hz, resulting in a maximum total response time of 50ms, which is much faster than the 100ms tactile simultaneity threshold so that no latency would be perceived by users [10, 41].

3.3 Motion Telemetry API

Games support motion platforms by exporting motion information in real-time via telemetry API so that motion platforms can react accordingly. Because we are effectively building a wearable motion simulator, we use the same mechanism to read the in-game motion data through the telemetry API via a UDP port [31]. We developed a Unity3D program (2019.4.10f) that reads acceleration, suspension information, and controller feedback intensity to compute the corresponding vibration pattern in either of our designs, converts the pattern to binary data that specifies the output intensity of each of the 16 LRAs, and sends the data to the control board via Wi-Fi.

doi:10.6342/NTU202203767

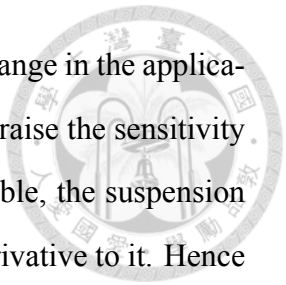

The telemetry data is processed at a rate of 25 Hz, so any subtle change in the application can be spotted immediately. However, such an update rate could raise the sensitivity to how noisy the data is. While the acceleration reading is rather stable, the suspension height data is quite noisy, and the issue gets worse when we take a derivative to it. Hence we applied the moving average filter of 100 ms window size to the signal of tire suspension height for denoising.

To access the feedback intensity in the controller, which is usually hidden from the user, we implement the Virtual Gamepad Emulation Framework [37] into our listener program. The framework creates a virtual controller connecting to the computer and provides several APIs to fake input or fetch feedback events. We used the virtual controller as the middle layer between the physical controller and the game application: we replicate all the inputs from the physical controller to the virtual one and assign the feedback intensity fetched from the virtual controller to the physical one. The player would notice nothing abnormal during the playthrough, and we may access the controller feedback intensity used in our [5] feedback design.

3.4 LRA Calibration

Because the actuators are placed around the head, the same LRA intensity may be perceived differently due to factors such as hair and curvature [34]. Furthermore, even the same batch of LRAs will have slight variances in their output. To ensure that each LRA is perceived to have identical intensity by the user, we developed a calibration process and iteratively improved it through our two formative studies.

Our current calibration process uses a 2-phase design. In the first phase, the front center LRA is used as the baseline, and users use an Xbox wireless controller's D-pad to move the target LRA to be calibrated (left/right) and adjust its intensity (up/down) to match the baseline. The baseline LRA and the target LRA would alternatingly vibrate for 0.5 seconds, ensuring that users can clearly perceive each LRA's intensity. The second phase is verification. The system iterates through all LRAs for users to double-check their calibration, and users can adjust as necessary.

doi:10.6342/NTU202203767

After completing calibration, we record all the intensity adjustments for each LRA. The adjustments are then normalized by dividing each by the maximum and then stored as percentage weights that will be multiplied when computing the final output. The calibration process typically takes 3-5 minutes and only needs to be performed once per user.

doi:10.6342/NTU202203767

Chapter 4

Vibrotactile Pattern Design

4.1 Design Process

We explored and iteratively refined our vibrotactile designs based on feedback from two formative studies. We will briefly summarize the design iterations but will focus on describing the current pattern design in detail in the rest of the section. Based on feedback from the first formative study, we removed vibration that corresponded to current speed, and increased the intensity of directional cues. Based on feedback from the second formative study, we applied low-pass filters to rough terrain, removed tactile motion from all acceleration and only used it for cold start, and added the *mirroring* approach.

4.2 Mirroring Approach

Haptic feedback is essential for immersive VR experiences; thus game designers and developers create well-designed controller-based haptic feedback. We propose a mirroring approach that takes existing controller haptic feedback and actuates the DrivingVibe headband accordingly. This allows games that do not support telemetry motion API, to support headset-based vibrotactile feedback.

Using one of the top-rated VR racing games, Assetto Corsa [1], as an example, we describe how we map its gamepad haptic feedback into feedback patterns for the headband.

[1] Assetto Corsa on SteamVR https://store.steampowered.com/app/244210/Assetto_Corsa/

doi:10.6342/NTU202203767

4.2.1 Gamepad Haptic in Racing Games

Modern gamepad and VR controllers use two embedded vibrotactile actuators to deliver a richer haptic experience than a single actuator. For example, Xbox ONE controllers use two ERM motors, DualSense™ wireless controllers use two LRA motors, and both HTC Vive controllers and Nintendo Switch Joy-Con controllers have a LRA in each of the left- and right-hand controllers. Since most controllers have haptic motors installed in a left-right manner, applications can create haptic events by simply specifying the intensity of the left or right motor without the need for customization to the controller type.

Although the algorithms to produce haptic feedback in a game are unknown outside of the game developers, we can still make some observations. The Assetto Corsa game is highly rated for its advanced physics engine and realistic visuals, and we analyze how it actuates the motors in the Xbox ONE controller, which has a low-frequency ERM motor on the left side and a high-frequency one on the right side.

From the subjective feeling, it seems that the game would actuate the low-frequency motor when the vehicle goes outside the track and the high-frequency one when the vehicle is accelerating, decelerating, or turning. This conjecture becomes more trustworthy when we combine the vibration intensity with in-game telemetry data. (Figure 4.1(a)(b))

While the intensity of the right motor reflects the magnitude of the G-force, the left motor is actuated either with 0% or 100% intensity (note that both intensity signals are convoluted with some wave signals).

4.2.2 Headband Intensity Mapping

Since we have the intensities of the actuators in the controller, we may just set the intensities of the headband motors with the same number. It might be intuitive to use the left motor's intensity to actuate the motors in the left half of the band, and so did the right half. However, we noticed that the actuators in the controller do not induce the feeling of directionality: it creates vibration throughout the whole chassis no matter which actuator is vibrating. Hence we decided to average the two intensities and broadcast to all the motors in the headband to mimic such sensation:

doi:10.6342/NTU202203767

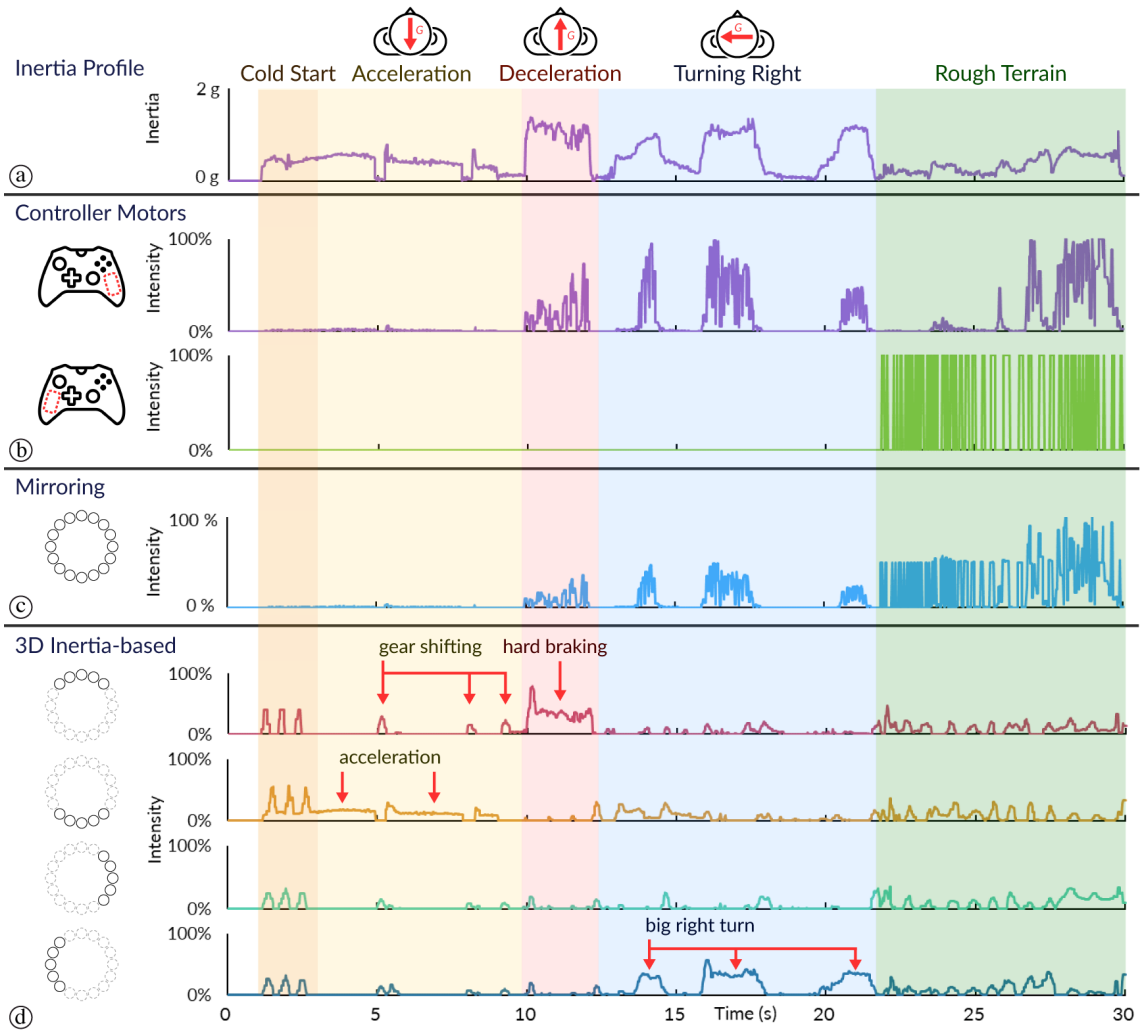

Figure 4.1: Different feedback designs gave the same driving behavior. (a) The profile of the magnitude of the inertia throughout the course. (b) The corresponding controller feedback intensity is built into the game. The right motor reacts to inertia, and the left motor reacts to the terrain. (c) The corresponding headband motor intensity in the mirroring approach. (d) The corresponding headband motor intensity in the approach. To show the directionality of this approach, we list the average intensity of the four quarters individually. The last part shows how *3D inertia-based* pattern reacts to rough terrains.

doi:10.6342/NTU202203767

$$\mathbf{I}_{motor} = \frac{\mathbf{I}_{left} + \mathbf{I}_{right}}{2}$$

Using this intensity mapping, the headband is literally a mirrored entity of the controller haptic (Figure 4.1(b)(c)). The major advantage of such mapping method is the universality, as it can also be used on most games, whenever there is the support of controller haptic feedback.

4.3 3D Inertia-based Approach

While the mirroring approach possess several advantages, it lacks directionality which has been shown to be effective in various scenarios [38, 31, 54, 5]. So we introduced a *3D inertia-based* approach that focuses on creating directional vibrotactile feedback. The goal of the feedback pattern design is to generate vibration information that can easily associate with motion events to enact sensorimotor contingency. Sensorimotor contingencies refer to a match of particular patterns from multisensory information caused by changed actions. For example, when the visual image of clapping fake hands is accompanied immediately by a tactile sensation in the hands, the multisensory impressions are closely correlated. Then the sensorimotor contingencies can be registered and result in rubber-hand illusion. Empirical evidence shows that subjects could experience ownership of virtual arms even with three times longer length than the real arm when the visuotactile congruence was built. [27] Sabine et al. further point out that augmenting non-realistic sensation in the body can also generate sensorimotor contingency. [28] They built a vibration belt that gives orientation information about the direction of magnetic north via vibrotactile stimulation on users' waists. Even the vibrotactile feedback is not an existing sensation in the body. After long-term training, users can utilize the belt's vibration as a body compass and increase users' navigational ability. Since the head vibration is also a non-realistic sensation, we will seek a more consistent and meaningful vibration pattern for our feedback design. This section detailed the motion event we chose and the algorithm to generate the vibrotactile patterns.

doi:10.6342/NTU202203767

4.3.1 Motion Events

The sense of acceleration, or inertia, is the most crucial component in the motion experience. Although humans can process inertia signals with the otolithic organs in the vestibular system [12], a further interpretation of the signals is acknowledged instead. It can be seen from previous research that users tend to associate haptic feedback with specific events such as accelerating or turning [31]. This gives the motivation to define *motion events*. *Motion events* are certain states that humans perceive and remember the most in motion experiences. For example, the most critical motion event in boating experiences might be the boat heaving.

To define the motion events for VR driving experiences, we listed the most vital scenarios based on human perception (Figure 1.1). In the prototype version, we first included *turnings*, *decelerations*, and *accelerations* which are the most common and frequent events in driving scenarios. In addition, we then chose car bumping due to *rough terrain* as our next candidate of events, as the whole vehicle body would shake drastically in the situation. Finally, we wish to utilize the apparent tactile motion to improve the pattern. After a process of deploying apparent tactile motion in several scenarios, we chose to apply it at the timing of *cold start*, which is the moment when the vehicle starts accelerating from being static.

4.3.2 Pattern Design

Prototype As a proof of concept, we first try to implement the feedback pattern of inertia events, which are *turnings*, *decelerations*, and *accelerations*, with the four ERM motors in the prototype stage (Figure 3.1(a)). In these events, we actuated the two motors, which represented the direction that the inertia pushed towards. For example, when in sudden braking, a huge forward inertia force would push the driver to the front. So the front two motors were actuated in *decelerations*, the back two motors were for *accelerations*, and the left / right two motors were for right / left *turnings*. To validate the choice of direction, we had an in-group pilot study that implemented the feedback as well as the inverse version into a racing track model made in Unity3D. All six participants agreed that the original

doi:10.6342/NTU202203767

version fits their expectations more and created more realism and immersion. Given the success of the prototype version, we extended the actuator count to 16 (Figure 3.1(b)(c)) and attempted to further explore a more sophisticated vibrotactile feedback design.

Directional Cue Design First, we wished to extend the prototype pattern that reflects several inertia events. Since *decelerations*, *accelerations*, and *turnings* can all be interpreted as the perceived inertia with different directions and magnitudes, we may directly associate the vibration pattern with the inertia vector. It is possible to render the direction of the inertia vector with 16 motors surrounding the head. HapticHead used 3-point head vibration to render the position of surrounding objects [23]. We first adapted this idea and used 2-point vibration. However, condensed vibration between two points would induce discomfort with high intensity. If we lower the intensity, the vibration is hard to notice instead. Thus we try to increase the vibration area and modify the intensities of each vibrator by linear mapping. After our pilot testing for different ranges of area, we found that 90°of width is both strong enough and comfortable.

For algorithm details, the explicit formula of intensity **I** at any moment is given by:

$$\mathbf{I}_{motor} = \max\left(0\%,\ \min\left(100\%\,,\frac{G_{now}-G_{lower}}{G_{upper}-G_{lower}}\right)\right)\times\left(100\%-\frac{\min(|\theta|,\ 45^\circ)}{45^\circ}\right)$$

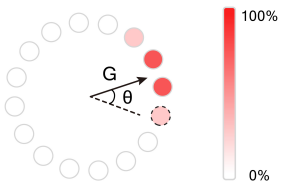

Figure 4.2: Schematic diagram of the directional cue design.

G_{lower} and G_{upper} stand for the lower threshold and the upper threshold to the magnitude of inertia, and θ stands for the angular distance from any certain motor to the direction of the inertia vector. We set a lower threshold of 0.1 g ($\approx 0.98 m/s^2$) and an upper thresh-

doi:10.6342/NTU202203767

old of 1.3 g ($\approx 12.74 m/s^2$). These thresholds were decided by the dynamic ranges of the inertia observed in the application. While the upper threshold defined when to max out the feedback intensity, the lower threshold could screen out the subtle noise to prevent overstimulation caused by overly frequent actuating. We used linear interpolation when the inertia was at intermediate values. The vibrators with an angular distance less than $45°$ will be activated with another interpolation on the intensity according to their angular distance to the direction of the inertia vector. The closer the vibrator is to the inertia, the higher intensity will be set. (Figure 4.2)

Rough Terrain Rendering Design We examined most of the physical parameters used in racing games to render the sensation of driving on rough terrains such as gravel roads or grass fields. First, we tried using the vertical acceleration of the vehicle, but it did not reflect the terrain condition well. Also, we observed that the vehicle would be severely shaking or tilting on rough terrains due to the unstable contact between the vehicle and the surface. Therefore we put our focus on the vehicle tires, which took just the roles of the contact points. It turned out that the suspension heights of the four tires can reflect terrain conditions the best. Suspension height is the distance between the tire touching ground and the underside of the vehicle chassis. Since the vehicle would be vertically unstable due to the coarse surface, the suspension height varies up and down drastically. Thus we used the derivative of the suspension height as the parameter representing the roughness of the road terrain.

We wish to mimic the sensation of instability in the tires, so we split the actuators into four regions, where the front-right corner corresponds to the front-right tire (Figure 1.1(b)) and so on. The four actuators at the exact front, back, left, and right are excluded to prevent the regions from overlapping and the whole band vibrating in certain situations so that the users may discriminate between the four tires.

For algorithm details, the explicit formula for intensity is given by:

$$\mathbf{I}_{motor} = \max\left(0\%,\ \min\left(100\%\ , \frac{\frac{dH}{dt} - H_{lower}}{H_{upper} - H_{lower}}\right)\right)$$

doi:10.6342/NTU202203767

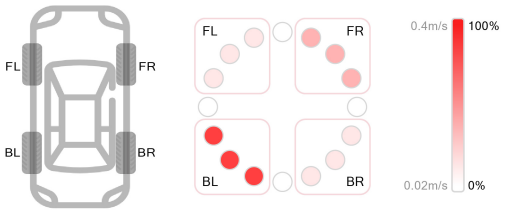

Figure 4.3: Schematic diagram of the directional cue design

Similar to the *Directional Cue* design, H_{lower} and H_{upper} stand for the thresholds to prevent overstimulation and set the max intensity. These values are found by observing the dynamic ranges in the application. By setting the lower threshold to 0.02 m/s, the actuators stay static when driving on the smooth track and start vibrating when driving on rough terrains such as grass fields. The intensity is again linearly interpolated for those between the two thresholds. (Figure 4.3)

Deploying Apparent Tactile Motion In the final stage of our pattern design, we decided to utilize the Apparent Tactile Motion (ATM) to further improve the experience. ATM is a tactile illusion created by controlling the time relations of two sequential tactile stimuli presented at separate locations on the skin to produce an illusion of a tactile movement between two points. [3] ATM had been shown to have the potential to create the sensation of wind pressure, and Chu et al. also suggested simulating air drag by continuous and multi-point vibration patterns [5]. This is similar to the special effects such as motion blur or speed lines that are added when the player accelerates in most racing games.

Two parameters can summarize the characteristic of ATM: 1) interstimulus onset interval (ISOI), which defines the delay between the start-up time of adjacent actuators [5], and 2) duration, which is how long a single actuator is stopped after its start-up. ISOI affects the traversing speed of ATM, and its value needs to lie in a specific interval, or the tactile illusion is destroyed. We adopted the symmetrical design and added in the property

doi:10.6342/NTU202203767

of continuity and multi-point, so multiple ATM would be produced continuously on both sides, creating the sensation of wind flowing.

To deploy ATM into VR driving experiences, we first considered several scenarios that coincided with high speed or accelerations. These attempts consisted of inducing ATMs when the driver is at a state of high velocity, high engine RPM, or acceleration. However, while these attempts did improve the experience at first, they started to cause overstimulation after long exposure to such feedback. “It just felt so busy on the head”, said a participant in our pilot testing. We also observed that ATM is hard to be related to physical parameters, as it acted like a special or unnatural effect. We conclude that ATM is more suitable for descriptive moments such as completing a lap, using power-ups, and accelerating from static. Finally, we decided to deploy ATM at the moment of *cold start*, which is the starting of the engine at a low temperature. We defined the *cold start* event as the short period when the vehicle starts accelerating from being static. Applying ATM at the start of the acceleration also improved the experience of acceleration since the users expect it to be a big moment, but the actual inertia is low (Figure 4.1(d)).

For algorithm details, we defined the *cold start* event by giving an acceleration of more than half-throttle when the velocity is less than 5 m/s. We set the ISOI at 100 ms according to the perceptual model [5], resulting in an angular speed of 0.625 rps. The duration is set to 300 ms or three-motor overlap in a single stroke of ATM. When the *cold start* events are detected, ATMs would be constantly produced at a rate of twice per second, or every 500 ms, from the front center and traverse through both sides of the head. We defined the interval by specifying the angular gap between two consecutive ATMs, so 500 ms resulted in a 45°gap or two motors of spacing. The interval can’t be lower than 300ms, or two ATMs would be inseparable, destroying the feeling. We tried different intervals and 500ms gives the best experience. There would be about six motors vibrating at the same time, so we set the intensity of each actuating motor at 40%.

Since we proposed three patterns in the *3D inertia-based* design, there would be multiple patterns operating at the same time. If a motor is responsible for multiple patterns, each pattern’s intensity would be summed up for the final output.

doi:10.6342/NTU202203767

Chapter 5

User Experience Evaluation

To evaluate the user experience of DrivingVibe designs, we selected one of the top rated VR racing game, Assetto Corsa [1], that supports telemetry API, has realistic audio-visual and physics, and has well designed haptic feedback. The built-in controller vibration will be used as a well-designed baseline, as well as the input source for the *mirroring* mode.

5.1 Experimental Design

This study uses a within-subject experimental design to compare the user experiences of three conditions: two DrivingVibe feedback patterns, *mirroring* and *3D inertia-based* designs, vs. a baseline. The baseline condition is the built-in controller vibration in driver mode, and no haptic feedback in passenger mode, as users are passive observers and controllers are not used.

We created a total of four tasks. The first three tasks are designed for users to experience specific types of motion events: 1) acceleration and deceleration (including cold start), 2) turning, and 3) rough terrain. These three are designed to be in passenger mode, in order to carefully control that all users experience the exact same motion experience. The fourth task is active free play in driver mode, when users freely drive around the course.

For each task, users experience the 3 feedback conditions, in counter-balanced order-

[1] Assetto Corsa on SteamVR https://store.steampowered.com/app/244210/Assetto_Corsa/

doi:10.6342/NTU202203767

ing. After each condition, users rated its immersion, realism, enjoyment, and comfort on a 7-point Likert scale. Specifically, the immersion and realism questions were adapted from the Presence Questionnaire (version 3)'s [60] questions 18 and 8.

At completing all conditions for all tasks, users chose their most preferred condition for immersion, realism, enjoyment, and overall preference. We prepared semi-structured interview questions to understand how the two pattern designs did or did not meet their expectations. We also asked them about the influence of the motor sound and whether they noticed the directionality feedback and tactile motion patterns.

5.1.1 Tasks 1-3: Passenger Mode

We implemented the passenger experience by using prerecorded clips with the replay function supported by the game. All 3 tasks started with the car being stationary and ended with braking to complete stop. The duration was chosen to be one minute to minimize motion sickness.

- Acceleration/Deceleration: was recorded on the Drag 2000m track. It included two full-throttle acceleration, two half-throttle acceleration, two full-brake deceleration, and two half brake deceleration.
- Turning: was recorded on the Vallelunga - Club track. It included two right turns and three left turns, spending about 33% of the time in the turns.
- Rough Terrain: was recorded on the Mugello Circuit track. The car was driving onto the grass field and then back on the road for four times, spending about 50% of the time on the grass field.

5.1.2 Task 4: Driver Mode

For free driving, we selected the Mugello Circuit track which has 15 turns and a long straight section, and the Lotus Elise SC car in gamer mode. An sample VR scene is shown in Figure 5.1(c), and to reflect typical gaming experience, the controller vibration feed-

doi:10.6342/NTU202203767

Figure 5.1: Passenger mode: (a) perspective in VR and (b) user; Driver mode: (c) perspective in VR and (d) user with controller.

back is on for all conditions. The task duration was extended to two minutes to allow participants time to experience different driving motions.

5.2 Participants and Procedure

We recruited 24 participants, 14 males and 10 females with age 20-43 (mean = 24.6, SD = 4.5), with Motion Sickness Susceptibility Questionnaire (MSSQ) scores below 70, which is the 80th percentile [13] to ensure that participants could finish the experiment without dropping out due of motion sickness. Participants all had normal or corrected-to-normal vision and had at least five real-world driving experiences in the past year. The experiment took approximately one hour and each participant received the equivalent of USD$6.5 compensation.

Upon participants' arrival, we explained the study procedure and measured their interpupillary distance (IPD) for HMD adjustment. We assisted participants to put on the Oculus Quest 2 HMD and the vibrotactile headband, in a seated position, as shown in Figure 5.1(b)(d). The driving game ran on a PC with an i5-11300H CPU, NVIDIA GeForce RTX 3060 Laptop GPU, and 24GB RAM. The study was conducted with the game's default sound effects without no background music to ensure that the experiment was close to a real driving experience.

Participants completed the calibration process, and could optionally reduce the overall intensity to 90% or 80% based on personal preference. After calibration, participants completed all four tasks, each consisted of three conditions in counter-balanced ordering. Participants rested for a few minutes between each condition to make sure that they felt no

doi:10.6342/NTU202203767

discomfort before the next trial. Participants could terminate the experiment at any time due to discomfort.

5.3 Analysis of Results

To compare the Likert ratings across three conditions, we first performed Friedman test then with Wilcoxon tests for pairwise post hoc analysis, with Bonferroni correction applied. Effect size of each comparison is calculated as $r = \frac{Z}{\sqrt{N}}$ [44].

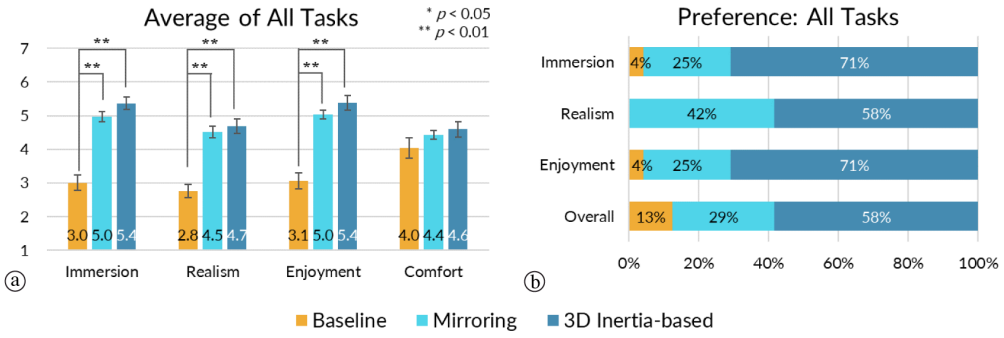

Figure 5.2: (a) Average scores of immersion, realism, enjoyment, and comfort on a 7-point Likert scale. This figure shows the scores averaged from the four tasks. Error bars represent SEM. (b) Preference rankings among all the tasks. The two feedback designs are preferred by at least 88% of the participants among comfort, realism, enjoyment, and immersion. The *3D inertia-based* condition is the most preferable.

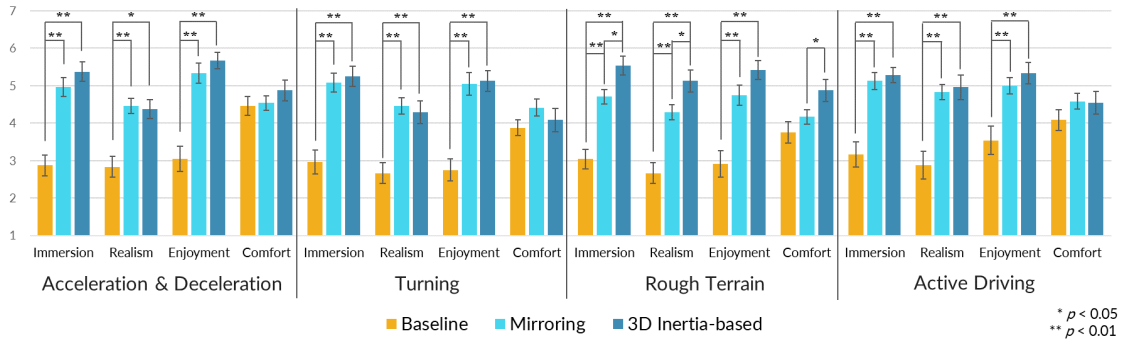

Figure 5.3: Average scores of immersion, realism, enjoyment, and comfort on a 7-point Likert scale in the four tasks. Error bars represent SEM.

doi:10.6342/NTU202203767

5.3.1 Likert-scale Ratings: Overall

Figure 5.2(a) shows the 7-point Likert-scale ratings averaged across all 4 tasks, showing that DrivingVibe designs have much higher ratings than the baseline for immersion, realism, and enjoyment. The *3D inertia-based* design had the highest ratings for all four dimensions, followed by the *mirroring* design, followed by the baseline.

Friedman tests show statistically significant differences between all the conditions in terms of immersion, realism, and enjoyment ($p < .00001$ for all), but no significance for comfort. Pair-wise comparison showed significant improvement for both DrivingVibe designs vs. baseline for immersion, realism, and enjoyment ($p < .01$ for all) with large effect sizes. However, no significant difference was found between the two DrivingVibe designs.

5.3.2 Likert-scale Ratings: By Task

Figure 5.3 shows the Likert-scale ratings for each of the 4 tasks. The statistically significant findings are generally consistent with the overall finding, that there was a significant improvement for both DrivingVibe designs vs. baseline for immersion, realism, and enjoyment ($p < .01$ for all) with large effect sizes.

Interestingly, it also shows that for the Rough Terrain task, the *3D inertia-based* design significantly improved immersion, realism, and comfort vs. the *mirroring* design ($p < .05$ for all), all with large effect sizes.

5.3.3 Preference across All Tasks

At the end of the study, after completing all tasks and conditions, participants were asked for their most preferred condition. As shown in 5.2(b), all participants preferred DrivingVibe over the baseline for realism (100%), with 96% for immersion and enjoyment, and 88% overall. Among those who preferred DrivingVibe, the *3D inertia-based* design was preferred for immersion (74%), realism (58%) and enjoyment (74%), and overall (66%).

doi:10.6342/NTU202203767

Chapter 6

Discussion

6.1 Connection between Vibration Feedback and Past Experience

All participants in our study have real-life driving experience, and most participants who rated higher realism in the DrivingVibe designs reported that they could associate vibration patterns with their past experience. All participants reported that the force feedback they received felt like real life driving experience in most driving events.

Although DrivingVibe designs can significantly improve the experience for most participants, some participants do not find differences between *mirroring* and *3D inertia-based* designs. Some participants reported "I think mirroring and 3D inertia-based are similar" (P1/3/5/6/13) in at least one driving event. Some participants relied on the feedback intensity to evaluate the vibrotactile feedback. "The intensity of mirroring/3D inertia-based is too big/small, so I think the other one is more realistic." (P1/12/17/18/19/22/24) is reported by part of the participants, but there was no trend on whether the design delivers more perceived intensity.

Regarding the *3D inertia-based* design, directionality is an essential factor that affects the experience. 15 out of 24 participants noticed the directionality with the *3D inertia-based* design, and all of them thought the directionality improves the experience. Some participants found the vibration pattern and reported that "It feels like the feeling of iner-

doi:10.6342/NTU202203767

tia." (P2/9). "Directionality makes me more comfortable." (P2/3) and"Directional vibration makes me turn my head." (P2, P10) are also notable replies. It shows that the inertia feedback might also be a cue to tell participants the turning directions.

Except for the first two tasks where inertia took the main part, directional feedback also provides benefits in simulating driving on rough terrain. For instance, "I can clearly feel the vibration of a single tire entering the grass field." (P6/7) and "I can feel the bumpiness in different directions." (P9/10) are reported in the interviews regarding *3D inertia-based* design, showing how directionality affects the user experiences. Directionality also allows us to give participants a more detailed haptic experience. In the two feedback designs, the vibration will occur continuously when the participants drive on rough terrains. We restrain the feedback area to the four corners in the *3D inertia-based* design, while in the *mirroring* design, the participants will withstand long-term vibrations all over the head. "I received excessive vibration when the car passes slightly over the rough terrain." (P5/12/17/18), "I received vibration around the head, but the constant vibration on the forehead is uncomfortable and unwarranted" (P22/23) and "The vibration is intermittent and weird." (P19/21) are reported in mirroring condition. With directional feedback design, we can create more detailed feedback and improve user experiences.

6.2 Vibration Noise in VR Driving

Since we put high-frequency motors around the head, caution was taken towards the vibration noise produced by the actuator. In the final interview, we asked the participants whether they heard any sound outside of the application and whether the sound would affect the experience. 11 out of 24 participants noticed the motor sound in the first place, and a total of 17 participants reported hearing the sound when we mentioned the motor sound, which is about 70% of the participants. Of the participants who noticed the vibration sounds, two participants reported "I think the vibration sound acts like the sound of a racing car." (P7/15), one participant reported "I think the vibration sound matches the sound of the game." (P9) and 7 participants reported that the vibration does not affect their experience negatively or some of them even neglect the sound when they start focusing

doi:10.6342/NTU202203767

on the VR experience. But there are still 7 participants who think the vibration sound is an interference, although such opinions do not affect their Likert score of comfort.

Based on the user feedback, we know that the motor noise would not destroy the experience when the sound is unnoticeable or matches the experience. Although our design did not take the motor noise into consideration, some participants have already rationalized motor noise in the game. Since vibration noise is practically inevitable, making it mentally acceptable is a reasonable approach. In most driving scenarios, motion events are usually accompanied by the engine or mechanical sounds. So if we could design the sound effects of the applications to be somewhat in harmony with the vibration noise, it might make the players tend to interpret the noise as a part of the game's sound effect. We proposed this idea to tackle the issue of actuator noise when implementing haptic feedback.

6.3 Improving Vibration Patterns

Although most of the feedback towards *3D inertia-based* design is positive, the performance of apparent tactile motion used in the *cold start event* did not meet our expectations. Only 4 out of 24 participants reported that they did feel the ATM throughout the user study. The other 9 participants just noticed something special but could not interpret it. We think that it might be because that ATM is a rather complicated vibrotactile feedback, and it needs more time or exposure for them to acknowledge the pattern. For improvement, we can try to improve the experience by deploying ATM in a more common event rather than once per drive-through.

We used linear mappings in the computation of intensity and frequency. However, the perception of motion signals are not likely to be linear but rather a more complex curve. For example, if a logistic curve that emphasizes the low level more is considered, the users may better feel the dynamic when the inertia is at an intermediate level.

To conclude, although no participant mentioned these slight differences in the study, there is still room for modification in the feedback pattern design.

doi:10.6342/NTU202203767

6.4 Extending DrivingVibe to Other VR Experiences

While significant improvement of motion sensation in driving experience was shown in this work, applications of other scenarios (e.g., skiing or skateboarding) could benefit from our feedback design. Combining our inertia-based event detection algorithm and a 16-LRA device, we can adapt our pattern design for other virtual motion experiences and improve realism. The motion events we explored are the most common in rapid-moving circumstances, while some scenarios like ski jumping, performing skateboard tricks, or riding a roller coaster contains events that involve vertical locomotion or self-rotation. The in-depth pattern design for these events is worth discussing.

6.5 Extending DrivingVibe to Other Parts of the Body

Three participants in the driver experience evaluation expected the vibrotactile feedback to be extended to different body parts, on the torso or the arms. Motion platforms can provide full-body motion simulation and thus obtain a high degree of immersion and realism. Previous works have explored the effect of tactile motion on various parts of the body, like back [21, 20], wrist [15], or forearm [20]. With prior knowledge of vibrotactile feedback on different body parts, expanding the stimulation area might be a method to further enhance the motion experience of DrivingVibe. For example, if the annular vibrator configuration is implemented on a belt, the same inertia-based pattern design can be replicated and provide motion cues around the waist. We used the derivative of suspension height to simulate the sensation of driving on rough terrain. Applying tactile motion vertically might also improve the experience of hitting road bumps. This can be achieved by extending the device down to the neck or the torso, providing more degrees of freedom of the tactile feedback.

doi:10.6342/NTU202203767

Chapter 7

Conclusion

We present DrivingVibe with two vibrotactile feedback patterns around the head to enhance VR driving experiences. We investigated whether our designed patterns can improve the realism, immersion, enjoyment, and comfort of the VR driving experience. The user experience evaluation showed that our patterns might successfully enact sensorimotor contingency to elicit an immersive and entertaining experience in a VR racing game and a 360° riding video. Furthermore, our vibration patterns do not reduce the user's comfort compared to the non-vibrotactile experience. On the contrary, we found the 3D inertia-based approach provide the best comfort in rough terrain scenario. We will investigate its effectiveness in reducing motion sickness in the future. To the best of our knowledge, this work is the first study on designing head vibrotactile patterns for VR racing games. The result could be used for further reference in designing haptic feedback for other gaming experiences.

doi:10.6342/NTU202203767

Bibliography

[1] M. Baarspul. A review of flight simulation techniques. *Progress in Aerospace Sciences*, 27(1):1–120, 1990.

[2] S. Beard, E. Buchmann, L. Ringo, T. Tanita, and B. Mader. Space shuttle landing and rollout training at the vertical motion simulator. In *AIAA Modeling and Simulation Technologies Conference and Exhibit*, page 6541, 2008.

[3] H. E. Burtt. Tactual illusions of movement. *Journal of Experimental Psychology*, 2(5):371, 1917.

[4] H.-Y. Chang, W.-J. Tseng, C.-E. Tsai, H.-Y. Chen, R. L. Peiris, and L. Chan. Facepush: Introducing normal force on face with head-mounted displays. In *Proceedings of the 31st Annual ACM Symposium on User Interface Software and Technology*, UIST '18, page 927–935, New York, NY, USA, 2018. Association for Computing Machinery.

[5] S.-Y. Chu, Y.-T. Cheng, S.-C. Lin, Y.-W. Huang, Y. Chen, and M. Y. Chen. Motionring: Creating illusory tactile motion around the head using 360° vibrotactile headbands. In *Proceedings of the 34st Annual ACM Symposium on User Interface Software and Technology*, 2021.

[6] M. Colley, P. Jansen, E. Rukzio, and J. Gugenheimer. Swivr-car-seat: Exploring vehicle motion effects on interaction quality in virtual reality automated driving using a motorized swivel seat. *Proc. ACM Interact. Mob. Wearable Ubiquitous Technol.*, 5(4), dec 2022.

doi:10.6342/NTU202203767

[7] F. Danieau, J. Fleureau, P. Guillotel, N. Mollet, A. Lécuyer, and M. Christie. Hapseat: Producing motion sensation with multiple force-feedback devices embedded in a seat. In *Proceedings of the 18th ACM Symposium on Virtual Reality Software and Technology*, VRST '12, page 69 – 76, New York, NY, USA, 2012. Association for Computing Machinery.

[8] V. Diener, M. Beigl, M. Budde, and E. Pescara. Vibrationcap: Studying vibrotactile localization on the human head with an unobtrusive wearable tactile display. In *Proceedings of the 2017 ACM International Symposium on Wearable Computers*, ISWC '17, page 82 – 89, New York, NY, USA, 2017. Association for Computing Machinery.

[9] H. Q. Dinh, N. Walker, L. F. Hodges, C. Song, and A. Kobayashi. Evaluating the importance of multi-sensory input on memory and the sense of presence in virtual environments. In *Proceedings IEEE Virtual Reality (Cat. No. 99CB36316)*, pages 222–228. IEEE, 1999.

[10] L. H. Frank, J. G. Casali, and W. W. Wierwille. Effects of visual display and motion system delays on operator performance and uneasiness in a driving simulator. *Human Factors*, 30(2):201–217, 1988. PMID: 3384446.

[11] R. Fukuyama and W. Wakita. An interactive flight operation with 2-dof motion platform. In *Proceedings of the 27th ACM Symposium on Virtual Reality Software and Technology*, VRST '21, New York, NY, USA, 2021. Association for Computing Machinery.

[12] J. M. Goldberg and C. Fernandez. Responses of peripheral vestibular neurons to angular and linear accelerations in the squirrel monkey. *Acta Oto-Laryngologica*, 80(1-6):101–110, 1975.

[13] J. F. Golding. Motion sickness susceptibility questionnaire revised and its relationship to other forms of sickness. *Brain Research Bulletin*, 47(5):507 – 516, 1998.

doi:10.6342/NTU202203767

[14] J. Gugenheimer, D. Wolf, E. R. Eiriksson, P. Maes, and E. Rukzio. Gyrovr: Simulating inertia in virtual reality using head worn flywheels. In *Proceedings of the 29th Annual Symposium on User Interface Software and Technology*, 2016.

[15] A. Gupta, T. Pietrzak, N. Roussel, and R. Balakrishnan. *Direct Manipulation in Tactile Displays*, page 3683 – 3693. Association for Computing Machinery, New York, NY, USA, 2016.

[16] S. Han, S. Mun, J. Seo, J. Lee, and S. Choi. 4d experiences enabled by automatic synthesis of motion and vibrotactile effects. In *Extended Abstracts of the 2018 CHI Conference on Human Factors in Computing Systems*, CHI EA '18, page 1–4, New York, NY, USA, 2018. Association for Computing Machinery.

[17] P. A. Hancock, D. A. Vincenzi, J. A. Wise, and M. Mouloua. *Human factors in simulation and training*. CRC Press, 2008.

[18] M. Hoppe, D. Oskina, A. Schmidt, and T. Kosch. Odin's helmet: A head-worn haptic feedback device to simulate g-forces on the human body in virtual reality. *Proc. ACM Hum.-Comput. Interact.*, 5(EICS), May 2021.

[19] J. Hosoi, Y. Ban, K. Ito, and S. Warisawa. Vwind: Virtual wind sensation to the ear by cross-modal effects of audio-visual, thermal, and vibrotactile stimuli. In *SIGGRAPH Asia 2021 Emerging Technologies*, SA '21 Emerging Technologies, New York, NY, USA, 2021. Association for Computing Machinery.

[20] A. Israr and I. Poupyrev. Control space of apparent haptic motion. In *2011 IEEE World Haptics Conference*, pages 457–462, 2011.

[21] A. Israr and I. Poupyrev. Tactile brush: Drawing on skin with a tactile grid display. In *Proceedings of the SIGCHI Conference on Human Factors in Computing Systems*, CHI '11, page 2019–2028, New York, NY, USA, 2011. Association for Computing Machinery.

[22] O. B. Kaul and M. Rohs. Haptichead: 3d guidance and target acquisition through a vibrotactile grid. In *Proceedings of the 2016 CHI Conference Extended Abstracts on*

doi:10.6342/NTU202203767

Human Factors in Computing Systems, CHI EA '16, page 2533–2539, New York, NY, USA, 2016. Association for Computing Machinery.

[23] O. B. Kaul and M. Rohs. Haptichead: A spherical vibrotactile grid around the head for 3d guidance in virtual and augmented reality. In *Proceedings of the 2017 CHI Conference on Human Factors in Computing Systems*, CHI '17, page 3729–3740, New York, NY, USA, 2017. Association for Computing Machinery.

[24] O. B. Kaul, M. Rohs, and M. Mogalle. Design and evaluation of on-the-head spatial tactile patterns. In *19th International Conference on Mobile and Ubiquitous Multimedia*, MUM '20, page 229–239, New York, NY, USA, 2020. Association for Computing Machinery.

[25] O. B. Kaul, M. Rohs, M. Mogalle, and B. Simon. Around-the-head tactile system for supporting micro navigation of people with visual impairments. *ACM Trans. Comput.-Hum. Interact.*, 28(4), jul 2021.

[26] O. B. Kaul, M. Rohs, B. Simon, K. C. Demir, and K. Ferry. Vibrotactile funneling illusion and localization performance on the head. In *Proceedings of the 2020 CHI Conference on Human Factors in Computing Systems*, CHI '20, page 1–13, New York, NY, USA, 2020. Association for Computing Machinery.

[27] K. Kilteni, J.-M. Normand, M. V. Sanchez-Vives, and M. Slater. Extending body space in immersive virtual reality: a very long arm illusion. *PloS one*, 7(7):e40867, 2012.

[28] S. U. König, F. Schumann, J. Keyser, C. Goeke, C. Krause, S. Wache, A. Lytochkin, M. Ebert, V. Brunsch, B. Wahn, et al. Learning new sensorimotor contingencies: Effects of long-term use of sensory augmentation on the brain and conscious perception. *PloS one*, 11(12):e0166647, 2016.

[29] J. Lee, J. Park, and S. Choi. Absolute and differential thresholds of motion effects in cardinal directions. In *Proceedings of the 27th ACM Symposium on Virtual Reality*

doi:10.6342/NTU202203767

Software and Technology, VRST '21, New York, NY, USA, 2021. Association for Computing Machinery.

[30] B. Lim, S. Han, and S. Choi. Image-based texture styling for motion effect rendering. In *Proceedings of the 27th ACM Symposium on Virtual Reality Software and Technology*, VRST '21, New York, NY, USA, 2021. Association for Computing Machinery.

[31] S.-H. Liu, P.-C. Yen, Y.-H. Mao, Y.-H. Lin, E. Chandra, and M. Y. Chen. Headblaster: A wearable approach to simulating motion perception using head-mounted air propulsion jets. *ACM Trans. Graph.*, 39(4), July 2020.

[32] K. Ly, P. Karg, J. Kreimeier, and T. Götzelmann. Development and evaluation of a low-cost wheelchair simulator for the haptic rendering of virtual road conditions. In *Proceedings of the 15th International Conference on PErvasive Technologies Related to Assistive Environments*, PETRA '22, page 32 – 39, New York, NY, USA, 2022. Association for Computing Machinery.

[33] B. Matthias, B. Florian, R. Till, and B. Michael. Proximityhat: a head-worn system for subtle sensory augmentation with tactile stimulation. In *Proceedings of the 2015 ACM International Symposium on Wearable Computers - ISWC '15*, pages 31 – 38. ACM Press, 2015.

[34] K. Myles, J. T. Kalb, J. Lowery, and B. P. Kattel. The effect of hair density on the coupling between the tactor and the skin of the human head. *Applied Ergonomics*, 48:177 – 185, 2015.

[35] F. Nakamura, A. Verhulst, K. Sakurada, M. Fukuoka, and M. Sugimoto. Virtual whiskers: Cheek haptic-based spatial directional guidance in a virtual space. In *SIGGRAPH Asia 2021 XR*, SA '21 XR, New York, NY, USA, 2021. Association for Computing Machinery.

[36] A. Nasser, K. Zheng, and K. Zhu. Thermearhook: Investigating spatial thermal haptic feedback on the auricular skin area. In *Proceedings of the 2021 International*

doi:10.6342/NTU202203767

Conference on Multimodal Interaction, ICMI '21, page 662–672, New York, NY, USA, 2021. Association for Computing Machinery.

[37] E. J. Nefarius, Kanuan. Virtual gamepad emulation framework, 2020.

[38] Y.-H. Peng, C. Yu, S.-H. Liu, C.-W. Wang, P. Taele, N.-H. Yu, and M. Y. Chen. *WalkingVibe: Reducing Virtual Reality Sickness and Improving Realism While Walking in VR Using Unobtrusive Head-Mounted Vibrotactile Feedback*, page 1–12. Association for Computing Machinery, New York, NY, USA, 2020.

[39] D. Pittera, D. Ablart, and M. Obrist. Creating an Illusion of Movement between the Hands Using Mid-Air Touch. *IEEE Trans Haptics*, 12(4):615–623, 2019.

[40] N. Ranasinghe, P. Jain, S. Karwita, D. Tolley, and E. Y.-L. Do. Ambiotherm: Enhancing sense of presence in virtual reality by simulating real-world environmental conditions. In *Proceedings of the 2017 CHI Conference on Human Factors in Computing Systems*, CHI '17, page 1731–1742, New York, NY, USA, 2017. Association for Computing Machinery.

[41] M. Rank, Z. Shi, H. J. Müller, and S. Hirche. Perception of Delay in Haptic Telepresence Systems. *Presence: Teleoperators and Virtual Environments*, 19(5):389–399, 10 2010.

[42] M. Rietzler, K. Plaumann, T. Kränzle, M. Erath, A. Stahl, and E. Rukzio. Vair: Simulating 3d airflows in virtual reality. In *Proceedings of the 2017 CHI Conference on Human Factors in Computing Systems*, CHI '17, page 5669–5677, New York, NY, USA, 2017. Association for Computing Machinery.

[43] J. M. Rolfe and K. J. Staples. *Flight simulation*. Number 1. Cambridge University Press, 1988.

[44] R. Rosenthal, H. Cooper, L. Hedges, et al. Parametric measures of effect size. *The handbook of research synthesis*, 621(2):231–244, 1994.

doi:10.6342/NTU202203767

[45] J. Schelter and F. Masi. Theater with seat and wheelchair platform movement, Nov. 3 1998. US Patent 5,829,201.

[46] J. Seo, S. Mun, J. Lee, and S. Choi. Substituting motion effects with vibrotactile effects for 4d experiences. In *Proceedings of the 2018 CHI Conference on Human Factors in Computing Systems*, CHI '18, page 1 – 6, New York, NY, USA, 2018. Association for Computing Machinery.

[47] V. Shen, C. Shultz, and C. Harrison. Mouth haptics in vr using a headset ultrasound phased array. In *Proceedings of the 2022 CHI Conference on Human Factors in Computing Systems*, CHI '22, New York, NY, USA, 2022. Association for Computing Machinery.

[48] Solla. Variable-lra-frequencies-on-drv2605, 2021.

[49] M. Sra, X. Xu, A. Mottelson, and P. Maes. Vmotion: Designing a seamless walking experience in vr. In *Proceedings of the 2018 Designing Interactive Systems Conference*, DIS '18, page 59–70, New York, NY, USA, 2018. Association for Computing Machinery.

[50] D. Stewart. A platform with six degrees of freedom. *Proceedings of the institution of mechanical engineers*, 180(1):371–386, 1965.

[51] Y. Tanaka, J. Nishida, and P. Lopes. Demonstrating electrical head actuation: Enabling interactive systems to directly manipulate head orientation. In *Extended Abstracts of the 2022 CHI Conference on Human Factors in Computing Systems*, CHI EA '22, New York, NY, USA, 2022. Association for Computing Machinery.

[52] Y. Tanaka, J. Nishida, and P. Lopes. Electrical head actuation: Enabling interactive systems to directly manipulate head orientation. In *Proceedings of the 2022 CHI Conference on Human Factors in Computing Systems*, CHI '22, New York, NY, USA, 2022. Association for Computing Machinery.

[53] T. Tanichi, F. Asada, K. Matsuda, D. Hynds, and K. Minamizawa. Kabuto: Inducing upper-body movements using a head mounted haptic display with flywheels. In

doi:10.6342/NTU202203767

SIGGRAPH Asia 2020 Emerging Technologies, SA '20, New York, NY, USA, 2020. Association for Computing Machinery.

[54] C.-M. Tseng, P.-Y. Chen, S. C. Lin, Y.-W. Wang, Y.-H. Lin, M.-A. Kuo, N.-H. Yu, and M. Y. Chen. Headwind: Enhancing teleportation experience in vr by simulating air drag during rapid motion. In *Proceedings of the 2022 CHI Conference on Human Factors in Computing Systems*, CHI '22, New York, NY, USA, 2022. Association for Computing Machinery.

[55] A. Väljamäe, P. Larsson, D. Västfjäll, and M. Kleiner. Travelling without moving: Auditory scene cues for translational self-motion. 2005.

[56] D.-B. Vo, J. Saari, and S. Brewster. Tactihelm: Tactile feedback in a cycling helmet for collision avoidance. In *Extended Abstracts of the 2021 CHI Conference on Human Factors in Computing Systems*, CHI EA '21, New York, NY, USA, 2021. Association for Computing Machinery.

[57] C. Wang, D.-Y. Huang, S.-w. Hsu, C.-E. Hou, Y.-L. Chiu, R.-C. Chang, J.-Y. Lo, and B.-Y. Chen. Masque: Exploring lateral skin stretch feedback on the face with head-mounted displays. In *Proceedings of the 32nd Annual ACM Symposium on User Interface Software and Technology*, pages 439–451, 2019.

[58] S. Weech, J. Moon, and N. F. Troje. Influence of bone-conducted vibration on simulator sickness in virtual reality. *PLOS ONE*, 13(3):1–21, 03 2018.

[59] A. Wilberz, D. Leschtschow, C. Trepkowksi, J. Maiero, E. Kruijff, and B. Riecke. Facehaptics: Robot arm based versatile facial haptics for immersive environments. In *Proceedings of the 2020 CHI Conference on Human Factors in Computing Systems*. ACM, 04 2020.

[60] B. G. Witmer, C. J. Jerome, and M. J. Singer. The Factor Structure of the Presence Questionnaire. *Presence: Teleoperators and Virtual Environments*, 14(3):298–312, 06 2005.

doi:10.6342/NTU202203767

[61] G. Yun, H. Lee, S. Han, and S. Choi. Improving viewing experiences of first-person shooter gameplays with automatically-generated motion effects. In *Proceedings of the 2021 CHI Conference on Human Factors in Computing Systems*, CHI '21, New York, NY, USA, 2021. Association for Computing Machinery.

doi:10.6342/NTU202203767

Appendix A

A.1 Details of the User Study Results

This appendix includes the analysis statistics in all the pairwise comparison as well as the preferences rankings collected in each of the task in the user experience evaluation study.

For Friedman tests, we reported the p-value as well as the Kendall's W value ($W = \frac{\chi^2}{N(K-1)}$) as the effect size. For Wilcoxon tests, we used $r = \frac{Z}{\sqrt{N}}$ as the effect size. Both effect size use the same interpretation guidelines of $0.1 \sim 0.3$ (small effect), $0.3 \sim 0.5$ (moderate effect), and ≥ 0.5 (large effect)

Table 1: Statistics of the analysis with the average scores among all tasks.

	$\chi^2{}_r$	p-value	W	Pairwise Comparison	Z	p-value	r
Immersion	39.52	<0.00001 **	0.82	Baseline < Mirroring	-4.29	<0.00001 **	0.87
				Baseline < Inertia	-4.29	<0.00001 **	0.87
				Mirroring < Inertia	-2.03	0.02118	0.44
Realism	31.00	0.00001 **	0.65	Baseline < Mirroring	-4.14	<0.00001 **	0.85
				Baseline < Inertia	-3.84	0.00006 **	0.78
				Mirroring < Inertia	-0.65	0.25785	0.14
Enjoyment	31.58	<0.00001 **	0.66	Baseline < Mirroring	-4.19	<0.00001 **	0.85
				Baseline < Inertia	-4.23	<0.00001 **	0.86
				Mirroring < Inertia	-1.47	0.07078	0.30
Comfort	3	0.22313	0.06	Baseline < Mirroring	–	–	–
				Baseline < Inertia	–	–	–
				Mirroring < Inertia	–	–	–

doi:10.6342/NTU202203767

Table 2: Statistics of the analysis in task 1

	χ^2_r	p-value	W	Pairwise Comparison	Z	p-value	r
Immersion	27.15	<0.00001 **	0.57	Baseline < Mirroring	-3.92	0.00004 **	0.88
				Baseline < Inertia	-4.01	<0.00001 **	0.88
				Mirroring < Inertia	-1.52	0.06426	0.36
Realism	18.15	0.00011 **	0.38	Baseline < Mirroring	-3.21	0.00066 **	0.66
				Baseline < Inertia	-2.69	0.00357 *	0.57
				Mirroring < Inertia	-0.40	0.34458	0.10
Enjoyment	28.31	<0.00001 **	0.59	Baseline < Mirroring	-4.01	<0.00001 **	0.88
				Baseline < Inertia	-4.01	<0.00001 **	0.88
				Mirroring < Inertia	-0.93	0.17619	0.23
Comfort	2.90	0.23506	0.06	Baseline < Mirroring	–	–	–
				Baseline < Inertia	–	–	–
				Mirroring < Inertia	–	–	–

Table 3: Statistics of the analysis in task 2

	χ^2_r	p-value	W	Pairwise Comparison	Z	p-value	r
Immersion	25.52	<0.00001 **	0.53	Baseline < Mirroring	-3.92	0.00004 **	0.88
				Baseline < Inertia	-3.96	0.00004 **	0.84
				Mirroring < Inertia	-0.58	0.28096	0.13
Realism	17.15	0.00019 **	0.36	Baseline < Mirroring	-3.72	0.0001 **	0.88
				Baseline < Inertia	-3.16	0.00079 **	0.69
				Mirroring < Inertia	-0.57	0.28434	0.13
Enjoyment	26.69	<0.00001 **	0.56	Baseline < Mirroring	-4.01	<0.00001 **	0.88
				Baseline < Inertia	-3.92	0.00004 **	0.88
				Mirroring < Inertia	-0.18	0.42858	0.04
Comfort	1.08	0.58178	0.02	Baseline < Mirroring	–	–	–
				Baseline < Inertia	–	–	–
				Mirroring < Inertia	–	–	–

Table 4: Statistics of the analysis in task 3

	χ^2_r	p-value	W	Pairwise Comparison	Z	p-value	r
Immersion	28.15	<0.00001 **	0.59	Baseline < Mirroring	-3.38	0.00036 **	0.72
				Baseline < Inertia	-4.08	<0.00001 **	0.88
				Mirroring < Inertia	-2.62	0.0044 *	0.60
Realism	19.31	0.00006 **	0.38	Baseline < Mirroring	-3.06	0.00111 **	0.64
				Baseline < Inertia	-3.71	0.0001 **	0.83
				Mirroring < Inertia	-2.27	0.0116 *	0.52
Enjoyment	16.90	0.00021 **	0.59	Baseline < Mirroring	-3.08	0.00104 **	0.69
				Baseline < Inertia	-3.67	0.00012 **	0.80
				Mirroring < Inertia	-2.07	0.01923	0.52
Comfort	7.75	0.02075 *	0.16	Baseline < Mirroring	-0.82	0.20611	0.18
				Baseline < Inertia	-2.00	0.02275	0.44
				Mirroring < Inertia	-2.30	0.01072 *	0.59

doi:10.6342/NTU202203767

Table 5: Statistics of the analysis in task 4

	χ^2_r	p-value	W	Pairwise Comparison	Z	p-value	r
Immersion	25.52	<0.00001 **	0.53	Baseline < Mirroring	-3.99	0.00003 **	0.85
				Baseline < Inertia	-3.61	0.00015 **	0.74
				Mirroring < Inertia	-1.22	0.11123	0.34
Realism	25.52	<0.00001 **	0.53	Baseline < Mirroring	-4.01	<0.00001 **	0.88
				Baseline < Inertia	-3.77	0.00008 **	0.79
				Mirroring < Inertia	-0.75	0.22663	0.19
Enjoyment	14.58	0.00068 **	0.30	Baseline < Mirroring	-3.36	0.00039 **	0.75
				Baseline < Inertia	-2.91	0.00181 **	0.65
				Mirroring < Inertia	-1.35	0.08851	0.32
Comfort	1.75	0.41686	0.04	Baseline < Mirroring	–	–	–
				Baseline < Inertia	–	–	–
				Mirroring < Inertia	–	–	–

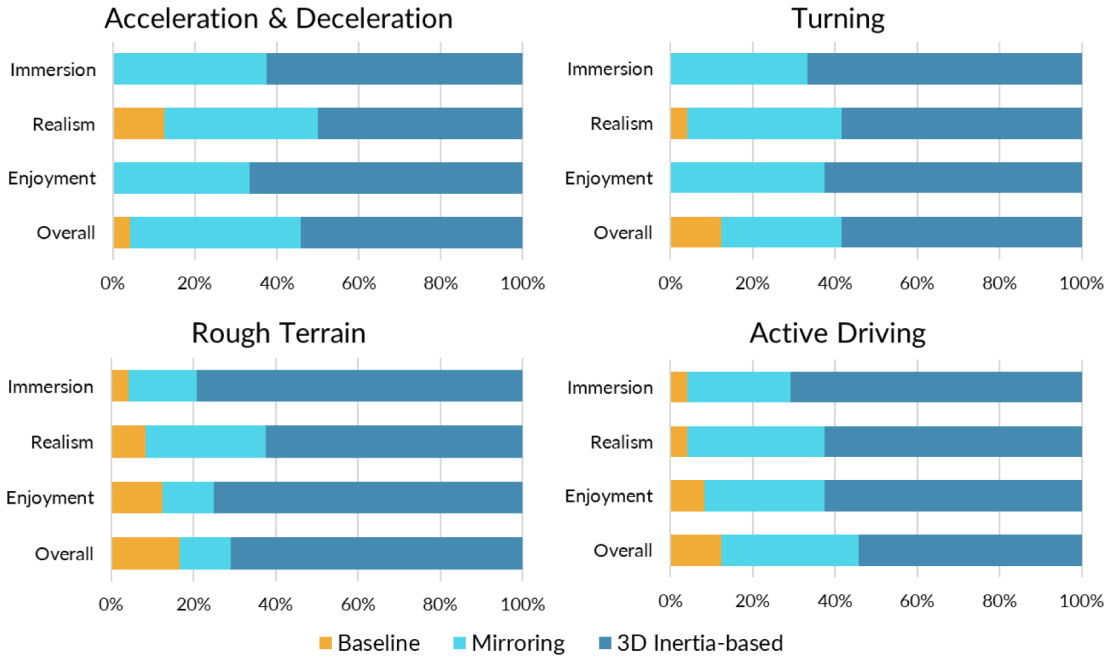

Figure 1: Preference rankings of immersion, realism, enjoyment, and overall in each of the task.

doi:10.6342/NTU202203767